

Method validation to assess in vivo cellular and subcellular changes in buccal mucosa cells and saliva following CBCT examination

Peer-reviewed author version

BELMANS, Niels; Gilles, Liese; Virag, Piroska; Hedesi, Mihaela; Salmon, Benjamin; Baatout, Sarah; Lucas, Stéphane; Jacobs, Reinhilde; LAMBRICHTS, Ivo & MOREELS, Marjan (2019) Method validation to assess in vivo cellular and subcellular changes in buccal mucosa cells and saliva following CBCT examination. In: DENTOMAXILLOFACIAL RADIOLOGY, 48 (6).

DOI: 10.1259/dmfr.20180428

Handle: <http://hdl.handle.net/1942/28106>

1 **Title**

2 Method validation to assess in vivo cellular and subcellular changes in buccal mucosa cells and saliva
3 following CBCT examinations

4

5

6

7

8

9

10

11

12

13

14

15

16

17

18

19

20

21

22

23

24

25

26

27

28 **Abstract**

29 *Objectives*

30 Cone-beam computed tomography (CBCT) is a medical imaging technique used in dental medicine.
31 However, there are no conclusive data available indicating that exposure to X-ray doses used by CBCT
32 are harmless. We aim, for the first time, to characterize the potential age-dependent cellular and
33 subcellular effects related to exposure to CBCT imaging. Current objective is to describe and validate the
34 protocol for characterization of cellular and subcellular changes after diagnostic CBCT.

35

36 *Methods*

37 Development and validation of a dedicated two-part protocol: 1) assessing DNA double strand breaks
38 (DSBs) in buccal mucosal (BM) cells and 2) oxidative stress measurements in saliva samples. BM cells and
39 saliva samples are collected prior to and 0.5 hours after CBCT examination. BM cells are also collected
40 24 hours after CBCT examination. DNA DSBs are monitored in BM cells via immunocytochemical staining
41 for γ H2AX and 53BP1. 8-oxo-7,8-dihydro-2'-deoxyguanosine (8-oxo-dG) and total antioxidant capacity
42 are measured in saliva to assess oxidative damage.

43

44 *Results*

45 Validation experiments show that sufficient BM cells are collected ($97.1\% \pm 1.4\%$) and that γ H2AX/53BP1
46 foci can be detected before and after CBCT examination. Collection and analysis of saliva samples, either
47 sham exposed or exposed to IR, show that changes in 8-oxo-dG and total antioxidant capacity can be
48 detected in saliva samples after CBCT examination.

49

50 *Conclusion*

51 The DIMITRA Research Group presents a two-part protocol to analyze potential age-related biological
52 differences following CBCT examinations. This protocol was validated for collecting BM cells and saliva
53 and for analyzing these samples for DNA DSBs and oxidative stress markers, respectively.

54

55 *Keywords*

56 Dental Cone-Beam Computed Tomography – DNA Double Strand Breaks – Oxidative stress – Buccal
57 mucosal cells - Saliva

58

59 **Introduction**

60 Dental cone-beam computed tomography (CBCT) is a relatively new and innovative diagnostic imaging
61 technique introduced in oral health care at the turn of the century.^(1, 2) Its growing use lies in the
62 diagnostic potential related to the transition from two-dimensional (2D) to three-dimensional (3D)
63 dentomaxillofacial diagnostic imaging.⁽³⁻⁶⁾ CBCT uses a cone-shaped X-ray beam and a 2D detector to
64 generate 3D images. Briefly, the source-detector rotates around the patient once, while generating a
65 series of 2D images. These images are then reconstructed into a 3D volume data set using a specialized
66 algorithm.^(3, 7-9) Specifically designed to produce cross-sectional images of the oral and maxillofacial
67 region, combined with its low cost and easy accessibility, CBCT technology has rapidly evolved in the
68 past decade. Nowadays it has become a widely available diagnostic tool for clinicians and has therefore
69 found applications in multiple dental specialties, including implant planning, endodontics, orthodontics
70 and maxillofacial surgery.^(1, 2, 4, 8, 10-12)

71 Like other medical imaging techniques, such as computed tomography (CT), CBCT uses X-rays for its
72 image acquisition. However, ionizing radiation (IR) is capable of damaging biomolecules (e.g. DNA or
73 proteins) directly or indirectly via the hydrolysis of water which generates free radicals, such as reactive
74 oxygen species (ROS).^(13, 14) Although CBCT is defined as a low dose imaging technique by the European
75 High-Level Expert Group on European Low Dose Risk Research (HLEG) (www.hleg.de), it is misleading to
76 see it as a 'low-dose' imaging modality just because it only takes one rotation compared to multiple
77 rotations in conventional CT. As in CT, the absorbed dose in CBCT heavily depends on selectable
78 exposure parameters that determine the image quality such as kVp, mAs, field of view (FOV), amount of
79 2D projections, reconstitution algorithm, etc..^(4, 15-18) Therefore, a wide range of CBCT doses is observed,
80 typically ranging from about 0.010 to 1.100 mSv per examination.^(15, 17-22) CBCT doses are lower than CT

81 doses (organ dose of about 15 mSv), however, they are higher than classical 2D dental radiography
82 techniques (organ dose of 0.001 – 0.1 mSv).^(4, 16, 23-26)

83 More recently, the dose of ionizing radiation delivered to pediatric patients has become a major concern
84 among clinicians worldwide.^(20, 24) In 2010, the New York Times was the first major newspaper to bring
85 this concern to the attention of the general public when they published the article entitled “Radiation
86 Worries for Children in Dentists’ Chairs”.⁽²⁷⁾ In practice, especially in orthodontics, a large portion of CBCT
87 examinations is performed on children (< 18 years old), who are known to be more radiosensitive than
88 adults.^(18, 28-30) These concerns about the dose, combined with an increasing amount of radiological
89 examinations annually, have led to questions about the biological uncertainties associated with
90 radiation-induced health risks at low doses in dental radiology.^(24, 31, 32)

91 Exposure to IR, such as X-rays, could result in damage to important biomolecules, either directly, but
92 mostly indirectly via generation of free radicals, usually through hydrolysis of water. These radicals (e.g.
93 reactive oxygen species (ROS)) can in turn damage biomolecules in nano- to microseconds.⁽¹⁴⁾ Since
94 more than 60% of a cell consists of water, most of the DNA damage is caused indirectly via ROS (e.g.
95 the hydroxyl radical, superoxide radicals and hydrogen peroxide).^(25, 33) An excess of ROS causes oxidative
96 stress. In the context of oral pathology, oxidative stress is associated with periodontitis, dental caries and
97 oral cancers.^(34, 35) ROS can cause oxidative DNA damage through oxidative base lesions, of which over
98 20 different lesions have been identified.⁽³⁶⁾ An example hereof is 8-oxo-7,8-dihydro-2'-deoxyguanosine
99 (8-oxo-dG), a mutagenic base modification.⁽³⁷⁾ Other types of DNA lesions include single strand breaks,
100 double strand breaks (DSBs) and base alterations.^(33, 38) DNA double strand breaks (DSBs) are the most
101 critical DNA lesions caused by IR. When not repaired correctly, DSBs can lead to chromosome
102 rearrangements, mutations and loss of genetic information.⁽³⁹⁻⁴⁴⁾ To protect themselves, eukaryotic cells
103 have developed the DNA damage response (DDR), a set of signaling and DNA repair pathways.⁽⁴⁵⁻⁴⁷⁾

104 Human buccal mucosa (BM) cells are useful for determining exposure to several environmental factors.⁽⁴⁸⁾
105 ⁴⁹⁾ Furthermore, BM cells are an easy accessible source of cells that can be sampled in a minimally invasive
106 way.^(50, 51) As such, they are being increasingly used to investigate the effects of exposure to genotoxins
107 that can cause DNA damage and cell death.^(48, 51, 52)

108 Another easy accessible biological sample is saliva, which, like BM cells, is easy to collect in an
109 inexpensive, painless and non-invasive way.⁽⁵³⁾ Known as the 'mirror of the body', saliva is finding its way
110 to research and the clinic as a diagnostic fluid.^(35, 54, 55) To date, the salivary metabolome has been
111 described and saliva has been used to link oxidative stress markers to several oral diseases, such as
112 dental caries and periodontitis.^(34, 35, 56)

113 Effective dose (ED), measured in mSv, is a dose quantity that takes following factors into account: 1) the
114 absorbed dose to all organs of the body, 2) the relative harm of the type of radiation, and 3) the
115 radiosensitivity of each organ. Although ED is an accepted term since its introduction in radiation
116 protection, it is often criticized. For example the weighing factors used to calculate the ED are determined
117 by scientific committees and may evolve over time.⁽⁵⁷⁻⁵⁹⁾ Furthermore, the ED is independent of gender
118 and age at exposure, whereas epidemiological data indicate that both gender and age at exposure are
119 important parameters.⁽⁶⁰⁾

120 A European project funded by the Open Project for European Radiation Research Area (OPERRA)
121 denoted as DIMITRA (Dentomaxillofacial Paediatric Imaging: An Investigation Towards Low Dose
122 Radiation Induced Risks) was initiated in order to characterize any potential cellular and subcellular
123 effects induced by dental CBCT imaging, with a focus on age- and gender specificity and with reference
124 to simulated ED (www.dimitra.be). *In vitro* results from DIMITRA were published previously, showing
125 transient increases in DNA DSBs and changes in inflammatory cytokines after CBCT exposure of dental
126 stem cells *in vitro*.⁽⁶¹⁾ The objective of the present report is to describe and validate a two-part protocol
127 enabling the DIMITRA project to assess the potential age-related cellular and subcellular effects using
128 DNA DSB detection in buccal mucosal cells and salivary oxidative stress measurement. To the best of
129 our knowledge, a protocol and method validation for characterizing cellular and subcellular effects of
130 CBCT exposure has not yet been described.

131

132 **Materials and methods**

133 ***Description of the DIMITRA protocol***

134 Synthetic swabs (EpiCentre®, Madison, USA) are used to collect BM cells from eligible patients. Eligibility
135 criteria are: having no systemic or acute diseases, taking no medication (antibiotics or anti-inflammatory
136 drugs), having a good oral hygiene and giving informed consent prior to conclusion. When eligible,
137 patients were asked to complete a questionnaire (supplementary data 1). At least one hour prior to BM
138 cell collection, subjects are asked not to eat, brush their teeth or smoke. Just before BM cell collection,
139 subjects rinse their mouth twice with water to remove excess debris. BM cells are collected from each
140 patient just before, 0.5 hours after and 24 hours after CBCT examination (fig. 1), using a protocol
141 modified from Thomas *et al.* (2009).⁽⁵⁰⁾ The 24 hours samples are collected at the patients' homes. To
142 this end patients receive detailed instruction sheets (supplementary data 2). After collection, samples are
143 sent to SCK•CEN via a professional courier service.

144

145 *Buccal mucosal cell collection and fixation*

146 Per patient six 15 ml conical tubes (Cellstar®, Greiner Bio-One, Vilvoorde, Belgium) (one for each time
147 point and cheek side) containing 10 ml of Saccomanno's fixative (SF) (50% ethanol, 2% polyethylene
148 glycol, 48% MilliQ water) are prepared. The swab is taken out of the package by the plastic handle. It is
149 important not to touch the swab itself. Then the swab is placed against the middle of the patient's cheek.
150 For reproducibility, the same cheek was used every time. Next, it is pressed firmly against the cheek and
151 moved in an upward-downward motion while turning the swab for at least 30 seconds. The swab is then
152 placed into SF in the 15 ml conical tube and shaken in such a manner that the cells are dislodged and
153 released into SF. The tubes are then stored at 4°C (for up to 7 days) before shipment to SCK•CEN by
154 courier service.

155 Within 7 days after sample collection, the BM cells are harvested from SF. For this purpose, the 15 ml
156 conical tubes are centrifuged at 580g for 10 minutes at room temperature (RT). The supernatant is
157 aspirated until about 1 ml is left. 5 ml of autoclaved buccal buffer (BuBu) (0.01 M Tris-HCl, 0.1 M EDTA,
158 0.02 M NaCl, 1% FBS, pH = 7) is added to the tube, after which the cells are vortexed briefly. Then, the
159 cells are centrifuged at 580g for 10 minutes at RT. The supernatant is removed completely and the cells
160 are washed with 5 ml BuBu and centrifuged at 580g for 10 minutes at RT. This washing step is repeated

161 twice to inactivate DNAses from the oral cavity and to remove excess debris and bacteria. After washing,
162 the supernatant is removed and the cells are resuspended in 5 ml of BuBu and vortexed briefly. Next,
163 the BM cells are passed through a 100 μ m nylon filter (Falcon®, VWR Belgium, Leuven, Belgium) into a
164 50 ml conical tube (Cellstar®, Greiner Bio-One, Vilvoorde, Belgium) to remove large aggregates of
165 unseparated cells. The 50 ml conical tube holding the filter is then centrifuged at 580g for 10 minutes at
166 RT. Afterwards, the BM cells in the filtrate are transferred to a new 15 ml conical tube. Then the BM cells
167 are centrifuged one last time at 580g for 5 minutes at RT. The supernatant is removed and the BM cells
168 are resuspended in 1 ml of BuBu. The BM cells are then centrifuged at 580g for 5 minutes at RT and the
169 supernatant is discarded afterwards. Then, the BM cells are fixed in 500 μ l of 2% paraformaldehyde (PFA)
170 (Sigma Aldrich, St-Louis, MO, USA) while vortexing the BM cells and adding the PFA dropwise. The BM
171 cells are incubated for at least 15 minutes at RT. After incubation, the BM cells are centrifuged at 580g
172 for 5 minutes. The supernatant is discarded and the BM cells are washed twice using 1x phosphate-
173 buffered saline (PBS) (Gibco, Life Technologies, Ghent, Belgium). After the last washing step, the BM cells
174 are resuspended in 1 ml 1x PBS. The BM cells can now be stored at 4°C for a longer period or used
175 immediately for immunocytochemical staining.

176

177 *Immunocytological staining for DNA double strand breaks: γ H2AX and 53BP1 staining*

178 Before immunocytochemical staining, the BM cells need to be transferred from the 15 ml conical tubes
179 to coverslips by cytocentrifugation. The BM cells are washed using 200 μ l of 1x PBS twice. During
180 washing, poly-L-lysine coated coverslips, which assure good attachment of the BM cells, are placed on
181 a microscope slide which is then inserted in a cytofunnel (ThermoFisher, Waltham, MA, USA). Next, 100
182 μ l of cell suspension is pipetted into each sample cup of a Cytofunnel. The cytofunnels are centrifuged
183 at 1200 rpm for 10 minutes in a cytocentrifuge (ThermoFisher, Waltham, MA, USA) at RT, causing the
184 BM cells to adhere to the coverslip inside the cytofunnel. After centrifugation, the coverslips are removed
185 and placed into a 4-well culture plate (Nunc, ThermoFisher Scientific, Roskilde, Denmark) so the BM cells
186 are facing up. The BM cells are allowed to air-dry for 2 minutes at RT.

187 Immunocytochemical staining was performed using a protocol as previously described by our group.⁽⁶²⁻
188 ⁶⁴⁾ First the BM cells are washed twice using cold 1x PBS for 5 minutes on a rocking platform. After
189 washing, the BM cells are permeabilized for 3 minutes using 0.25% Triton X-100 in 1x PBS at RT. Next,
190 the BM cells are washed three times with 1x PBS. Then the BM cells are blocked with 1x pre-immunized
191 goat serum (ThermoFisher Scientific, Waltham, MA USA) in a solution of 1x TBST, 0.005 g/v% TSA
192 blocking powder (PerkinElmer, FP1012, Zaventem, Belgium) (TNB) for 1 hour at RT. After blocking the
193 primary mouse monoclonal anti- γ H2AX antibody (Millipore 05-636, Merck, Overijse, Belgium) (1:300 in
194 TNB) and rabbit polyclonal anti-53BP1 antibody (Novus Biologicals NB100-304, Abingdon, UK) (1:1000
195 in TNB) are added. Next, the BM cells are incubated overnight at 4°C on a rocking platform. After
196 incubation, the BM cells are washed three times with 1x PBS. Then the secondary goat anti-mouse Alexa
197 Fluor® 488-labeled antibody (1:300 in TNB) and goat anti-rabbit Alexa Fluor® 568-labeled antibody
198 (1:1000 in TNB) (ThermoFisher Scientific, A11001, Waltham, MA USA) were added. The BM cells are
199 incubated for 1 hour on a rocking platform in the dark. Afterwards, the BM cells are washed twice using
200 1x PBS. Next, slides are mounted with ProLong Diamond antifade medium with 4',6-diamidino-2-
201 phenylindole (DAPI) (ThermoFisher Scientific, Waltham, MA USA).

202 Finally, images are acquired with a Nikon Eclipse Ti fluorescence microscope using a 40× dry objective
203 (Nikon, Tokyo, Japan). Images are analyzed using open source Fiji software.⁽⁶⁵⁾ The software allows to
204 analyze each nucleus based on the DAPI signal. Within each nucleus, the intensity signals from the Alexa
205 488 and Alexa 568 fluorochromes are analyzed after which the number of co-localized γ H2AX and 53BP1
206 foci per nucleus are determined in an automated manner using the Cellblocks toolbox (fig. 2).⁽⁶⁶⁾

207

208 *Saliva collection and analysis*

209 Saliva samples are collected right before and 0.5 hours after CBCT examination (fig. 1) using the passive
210 drool method, which is considered to be the 'gold standard' for saliva sampling.⁽⁶⁷⁾ As with the BM cells
211 (saliva is sampled at the same time), subjects are asked not to eat, brush their teeth or smoke one hour
212 prior to saliva sampling. Just before saliva collection, subjects will rinse their mouth twice with water to
213 remove excess debris. If blood is detected in the saliva, the sample is not included for this study. The

214 saliva samples will be stored at -20°C immediately after collection before shipment to SCK•CEN by
215 courier service. Once at SCK•CEN samples will be centrifuged at 10 000g at 4°C to remove most of the
216 mucus and the supernatant will be stored at -80°C. The stored samples will be used to determine 8-oxo-
217 dG concentrations and the total antioxidant capacity (fig. 2).

218

219 *8-oxo-dG determination*

220 8-oxo-dG concentrations will be determined by competitive enzyme-linked immunosorbent assay
221 (ELISA) (Health Biomarkers Sweden AB, Stockholm, Sweden). To remove substances other than 8-oxo-
222 dG which could cross-react with the monoclonal antibody used in the ELISA-kit, 800 µL sample will be
223 purified prior to ELISA using a C18 solid phase extraction column (Varian, Lake Forest, CA, USA) after
224 which the samples are freeze-dried. This purification is performed twice.⁽⁶⁸⁾

225 The 8-oxo-dG concentration of saliva will be measured based on a modified ELISA protocol provided by
226 Health Biomarkers Sweden AB (Stockholm, Sweden). The protocol will be performed as previously
227 described by Haghdoost *et al.*⁽⁶⁹⁾ Briefly, 270 µL of purified sample/standard will be mixed with 165 µL of
228 primary antibody (80 ng/ml) mix in Eppendorf tubes. Next the samples will be incubated for 2 hours at
229 37°C. During incubation, the ELISA plate will be washed twice using 1x PBS. After incubation 140 µL of
230 sample/standard will be loaded onto the plate in triplicate. The plate will be incubated overnight at 4°C
231 on a horizontal shaker. Next the plate will be washed three times using 1x washing solution. After
232 washing 140 µL of secondary antibody mix is added to each well. The plate is incubated for 2 hours at
233 RT on a horizontal shaker. Next the plate is washed three times with 1x washing solution and once more
234 with 1x PBS. Finally, the reaction is visualized by the addition of 140 µL chromogenic substrate 3,3',5,5'-
235 Tetramethylbenzidine (One-Step substrate system; Dako, Glostrup Municipality, Denmark), and further
236 incubation in the dark for 15 minutes. The reaction is stopped by adding 70 µL of 2M H₂SO₄. The
237 absorbance is measured at 450 nm (signal) and 570 nm (background) using a microplate reader
238 (ClarioStar, BMG Labtech, Ortenberg, Germany) (fig. 2).

239

240 *Total antioxidant capacity*

241 To determine the antioxidant capacity of saliva samples, the ferric reducing antioxidant power (FRAP)
242 assay is used (Cell Biolabs, CA, USA). The FRAP assay will be performed according to the manufacturer's
243 instructions. Briefly, per well of a 96-well plate 100 μ l of sample/standard and 100 μ l of reaction reagent
244 are added. Next the samples/standards are incubated for 10 minutes at RT on a horizontal shaker. Finally,
245 the absorbance will be measured at 560 nm using a microplate reader (ClarioStar, BMG Labtech,
246 Ortenberg, Germany). The results will be expressed as Iron(II) concentration (μ M) or FRAP value (fig. 2).

247

248 **Protocol validation**

249 *Pilot study population*

250 Healthy adults (N = 6) are included in this pilot study to validate the DIMITRA study protocol. These
251 patients are referred for a CBCT examination. All patients were asked to sign informed consent forms
252 prior to being included in the study. The validation study was approved by the ethical committees of the
253 participating hospitals, since this is part of the scope of the DIMITRA study.

254

255 *Flow cytometrical identification of buccal mucosal cells*

256 Cells collected using the method described earlier are identified with the epithelial cell marker
257 cytokeratin 4 (CK4) and lymphoid cell marker CD45 to identify the amount of BM cells collected with the
258 swab. A431 and PC3 (courtesy of Katrien Konings) cell lines are used as a positive control for CK4
259 expression. Jurkat cells are used as a positive control for CD45 expression.

260 All cells are washed with 1xPBS and fixed in ice-cold (-20°C) 70% ethanol at a concentration of 1×10^6
261 cells/ml or 2×10^6 cells/ml (Jurkat). Next, cells are washed once with a solution of 1x PBS, 5% FBS (GIBCO,
262 Life Technologies, Ghent, Belgium) and 0.25% Triton X-100 (Sigma-Aldrich chemistry, St-Louis, MO USA)
263 (PFT) and are then blocked for 1h at RT in PFT. After blocking, cells are incubated with a rabbit anti-CK4
264 antibody (diluted 1:100 in PFT) overnight at 4°C on a horizontal shaker. Next, cells are washed twice with
265 PFT. Subsequently, Alexa 488-conjugated donkey anti-rabbit secondary antibody (diluted 1:200 in PFT)
266 and primary mouse anti-human CD45 antibody labelled with allophycocyanin (diluted 1:50 in PFT) are
267 added and the cells were incubated for 2h at RT in the dark. After incubation, the cells are washed twice

268 with PFT and treated with 10 µg/ml of the DNA dye 7-AminoActinomycin D (7-AAD) for 15 min at RT. 7-
269 AAD is used to distinguish cellular material from debris. Furthermore, it gives information about the
270 current cell cycle phase of the samples. Finally, the samples are filtered on a BD conical tube (Falcon ®,
271 Corning, NY, USA) and analyzed on the BD Accuri™ C6 Flow Cytometer (BD Biosciences, San Jose, CA
272 USA). At least 10.000 events are measured. Single-colour stained cells are included for colour
273 compensation. Gating is based on using A431, PC3 and Jurkat cells as positive/negative control for CK4
274 or CD45. Cells in G₁/G₀ phase and CK4⁺ are identified as BM cells.

275

276 *Histological staining for epithelial cell identification*

277 Cells are collected using the method described earlier and were stained using Giemsa to allow for
278 histological examination of the cells collected in the swab. After the cells are fixed in 2% PFA, they are
279 spotted on poly-L-lysine coated coverslips (see above). Next, the cells are stained with Giemsa (1:50 in
280 0.2M acetate buffer, pH = 3.36) (VWR International, Radnor, PA, USA) for 1 hour at RT. After incubation,
281 the cells are washed twice with milliQ water. Next, the slides are mounted with DPX (VWR International,
282 Radnor, PA, USA). Finally, images are acquired with a Nikon Eclipse Ti microscope using a 20× dry
283 objective for brightfield image acquisition (Nikon, Tokyo, Japan).

284

285 *Statistics*

286 Statistical analyses is performed using GraphPad Prism 7.02 (GraphPad Inc., CA, USA). Induction of DNA
287 DSBs in BM cells is analyzed using repeated measures ANOVA. Both 8-oxo-dG concentrations and FRAP
288 values before and after CBCT are compared using a paired t-test. To perform the above listed parametric
289 tests, values should be normally distributed and the variances should be equal. Should these conditions
290 not be met, non-parametric alternatives are used. P values lower than 0.05 are considered as statistically
291 significant. Age-related effects are not considered during the validation experiment.

292

293 **Results**

294 Validation of the described protocol was performed on samples collected from adults (Table 1). BM cells
295 were collected from adult volunteers (n = 6) using buccal swabs. Characterization of the cells collected
296 by the swabs was performed using flow cytometrical and light microscopical analysis. CK4⁺ cells (that
297 were in G₁/G₀ phase) were identified as BM cells. Flow cytometrical analysis showed that 97.1% ± 1.4%
298 of the cells were CK4⁺ BM cells, whereas less than 1% of cells were CD45⁺. These CD45⁺ cells are most
299 likely leukocytes (fig. 3). Further histological analysis confirmed that the collected cells are indeed BM
300 cells, in various stages of exfoliation: some are nucleated, while others are not (fig. 4A, arrowheads).

301 The presence of DNA DSBs in BM cells was detected using an immunocytochemical staining for γH2AX
302 and 53BP1 (fig. 4B-E). Analysis of colocalized γH2AX and 53BP1 foci shows that 0.015 ± 0.012 foci/nuclei
303 were counted before CBCT and 0.028 ± 0.028 foci/nuclei were counted after (p = 0.99).

304 Saliva samples were collected from adults that were subjected to CBCT examination twice: once without
305 IR exposure (sham control = group 1) and once with IR exposure (= group 2). These samples (n = 5)
306 were used to validate the protocols for the 8-oxo-dG and FRAP determination.

307 The change in 8-oxo-dG levels before and after CBCT exposure between group 1 and group 2 was
308 compared. Group 1 showed no difference (-0.09 ± 0.44 ng/ml; p = 0.88) in 8-oxo-dG levels whereas an
309 increasing trend was found in group 2 (2.5 ± 3.0 ng/ml; p = 0.19). Comparison of the changes in both
310 groups was not significant (p = 0.15), but it shows that after IR exposure (due to CBCT examination)
311 changes in 8-oxo-dG levels can be detected.

312 In combination with the 8-oxo-dG ELISA, a FRAP assay was performed. When comparing FRAP values
313 before and after CBCT examination, results show that the FRAP value does not change in group 1 (-3.6
314 ± 69; p > 0.99), but there is a decreasing trend in group 2 (-18 ± 49; p = 0.31). The change between both
315 groups does not differ significantly (p = 0.89), but these data show that after IR exposure (due to CBCT
316 examination) changes in FRAP values can be detected.

317

318 **Discussion**

319 Currently, the main challenge in the field of radiation protection is identifying biomarkers that allow
320 detection of cellular and subcellular changes due to exposure to low doses of IR (< 0.1 Gy). These

321 biomarkers could then be used to predict low dose IR-associated risks. To this end, blood is the most
322 commonly used sample to study cellular and subcellular changes in the low dose range, such as the
323 doses used in medical diagnostic imaging. Blood contains numerous cells that can be used for a variety
324 of assays used in low dose radiation research, such as the micronucleus assay, dicentric assay, comet
325 assay, γ H2AX assay, oxidative stress tests (e.g. 8-oxo-dG) and even gene expression assays.⁽⁷⁰⁻⁷⁶⁾ The
326 advantage of blood sampling is that a standardized protocol can be used, the procedure is easy and
327 small volumes suffice for most tests performed. However, the major limitation of drawing blood is that
328 the procedure is invasive, which can cause discomfort to the patient, especially to pediatric patients.⁽⁷⁰⁾
329 The DIMITRA Research Group provides a two-part protocol to assess potential cellular and subcellular
330 effects after exposure to low doses of IR, i.e. CBCT examinations. This protocol focusses on non-invasive
331 samples, i.e. BM cells and saliva samples. Compared to blood samples, BM cells and saliva samples have
332 several major advantages: collection is non-invasive, cheap, painless and therefore allows easy repeated
333 sampling.^(50, 51, 53) This opens new opportunities for use in (oral) healthcare with an increased suitability
334 when pediatric patients are involved. The two-part protocol focusses on detection of DNA DSBs and
335 oxidative stress markers. Oxidative stress can induce oxidative DNA damage which has mutagenic and
336 tumorigenic potential.⁽⁷⁷⁾ DNA DSBs, which can (partly) be caused by oxidative stress, is associated with
337 carcinogenesis, an important health risk related to IR exposure.^(78, 79) Therefore, DNA DSB formation and
338 repair are important markers to assess potential health risks in patients exposed to IR.

339 The current paper describes and validates this two-part protocol. The collection method for BM cells was
340 validated by flow cytometry (presence of G_1/G_0 phase CK4⁺ cells) and light microscopy (Giemsa staining).
341 BM cells from different mucosal layers were collected, although the majority of the cells were nucleated.
342 These results show that this collection method yields sufficient BM cells for microscopical analysis. The
343 use of γ H2AX foci in BM cells is described before as is the use of a γ H2AX/53BP1 immunofluorescent
344 staining for the detection of DNA DSBs. ^(51, 64, 80-82) However, to the best of our knowledge, this is the first
345 time that a protocol is proposed to detect DNA DSBs after CBCT examination, although other
346 genotoxicity markers have been published before.⁽⁸³⁾ Our validation data show that that *ex vivo* BM cells
347 can be used to perform γ H2AX/53BP1 analysis. Future studies will investigate whether age-dependent

348 differences can be detected in the amount of DNA DSBs after CBCT examination. For saliva collection, a
349 protocol was described based on the passive drool method, after which the samples are immediately
350 stored at -20°C. Comparison between sham exposure and IR exposure, i.e. CBCT examination, shows that
351 changes in 8-oxo-dG and FRAP levels can be detected in saliva samples after CBCT examination. These
352 findings confirm that the methods described in this paper are suited for evaluating potential effects of
353 low dose IR exposure in BM cells and saliva samples. The changes detected here are small, but can be
354 attributed to the age of the volunteers: adults are more radioresistant than children, therefore we
355 hypothesize that the effects of low dose IR exposure might be greater in children.

356 Despite the aforementioned advantages and validation of the DIMITRA study protocol, some
357 precautions should be taken into account when using BM cells and saliva. BM consists of several layers
358 of cells, thus sampling should be done in an uniformed way to avoid differences in cell type distribution.
359 For example, it is known that the amount of basal cells increases when the cheek is sampled
360 repeatedly.^(48, 50) Therefore, the authors suggest to collect some test samples prior to the actual study
361 and to characterize the cells that are collected, as described earlier. Although cigarette/cigar smoke is a
362 known cytotoxin and genotoxin to BM cells⁽⁸⁴⁾, one limitation of this validation protocol is that 'smoking'
363 was not included in the exclusion criteria. Therefore, it is recommended to add 'smoking' as an exclusion
364 criterion when conducting studies in which BM cells are collected for this type of study.

365 Saliva composition can be affected by several factors, such as the collection itself, time of day, intake of
366 antioxidants, time since tooth-brushing, presence of blood, drug intake, etc.. Moreover, some (pediatric)
367 patients might not be able to produce (enough) saliva spontaneously. However, the authors recommend
368 to not induce salivation actively, since this will create a bias when compared with spontaneous
369 salivation.⁽³⁵⁾ To keep this type of bias to a minimum, our protocol is based on the passive drooling
370 method to collect saliva, which is regarded as the gold standard.⁽⁶⁷⁾ Additional information from the
371 patients on drug intake, previous radiation exposure, etc. should be obtained as well through a
372 questionnaire.

373 For the post-imaging assessment, 30 minutes and 24 hours were chosen for γ H2AX/53BP1 staining
374 based on previous results from SCK•CEN, in which the peak response is seen after 30 to 60 minutes and

375 most DNA damage is resolved after 24 hours.⁽⁶²⁻⁶⁴⁾ For the 8-oxo-dG analysis and FRAP assay, we chose
376 time points based on Haghdoost *et al.*, who tested 8-oxo-dG after 30 minutes.⁽⁶⁹⁾ This coincides with BM
377 cell sampling, which is an advantage since this way DNA DSB and 8-oxo-dG levels can be correlated. The
378 results show that changes, especially in oxidative stress markers, can be detected at this time. However,
379 it is possible that the selected time points are not the most optimal ones. Finally, we are not certain that
380 the described methods for detecting DNA damage will be sensitive enough to detect changes following
381 CBCT examination in children, since to the best of the authors' knowledge, this type of study has not
382 been performed before. Current time points are selected based on literature, as mentioned above, but
383 also out of practical consideration: i.e. not letting the patient wait too long after the CBCT examination.
384 If necessary, and if patients are willing, it may be possible to include additional time points (e.g. 60
385 minutes after CBCT examination).

386 The DIMITRA study protocol presented here is designed to be cost effective, quick, painless and non-
387 invasive. The use of this protocol, however, is not limited to this study and can be easily implemented in
388 other (radio)biological studies. For example, this protocol can be used in a similar setting in which
389 patients are exposed to a head and neck CT, or in cancer patients treated for head and neck cancer.
390 Furthermore, the use of saliva can be used to monitor patients exposed to short- and long-lived
391 radionuclides for diagnostics/therapy. These examples expand the use of this protocol from risk
392 assessment in medical diagnostics, to follow-up/monitoring of radiotherapy patients, two distinctive
393 field in medicine using ionizing radiation.

394

395 **Conclusion**

396 It is well-known that children are more radiosensitive than adults. Together with the increasing amount
397 of radiological examinations annually, this has recently led to societal concerns about exposure to IR
398 during medical procedures. The DIMITRA Research Group presents a dedicated, two-part protocol to
399 analyze potential age-related biological differences in response to CBCT examinations in both pediatric
400 and adult patients. This protocol was validated for collecting BM cells and saliva, as well as for analyzing
401 BM cells and saliva samples for DNA damage and oxidative stress markers, respectively. After validation

402 in this paper, this dedicated protocol can be used in different age categories to detect potential cellular
403 and subcellular effects following dental CBCT imaging.

404

405 **Acknowledgements**

406 The DIMITRA Research Group that contributed to this paper consists of N. Belmans, M. Moreels, S.
407 Baatout, B. Salmon, A.C. Oenning, C. Chaussain, C. Lefevre, M. Hedesiu, P. Virag, M. Baciut, M. Marcu, O.
408 Almasan, R. Roman, I. Barbur, C. Dinu, H. Rotaru, L. Hurubeanu, V. Istouan, O. Lucaciu, D. Leucuta, B.
409 Crisan, L. Bogdan, C. Candea, S. Bran, G. Baciut, R. Jacobs, H. Bosmans, R. Bogaerts, C. Politis, A. Stratis,
410 R. Pauwels, K. de F. Vasconcelos, L. Nicolielo, G. Zhang, E. Tijskens, M. Vranckx, A. Ockerman, E. Claerhout,
411 E. Embrechts.

412

413 **Figures**

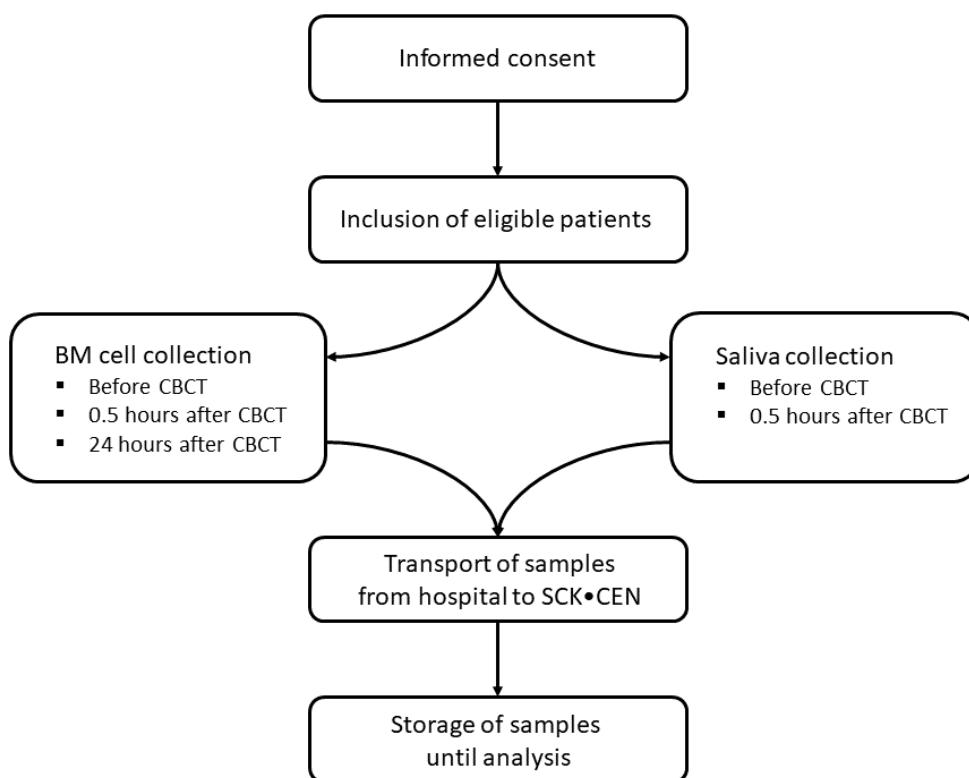


Figure 1. Flow chart for patient inclusion and patient sampling. *CBCT = Cone Beam Computed Tomography; BM = Buccal mucosa*

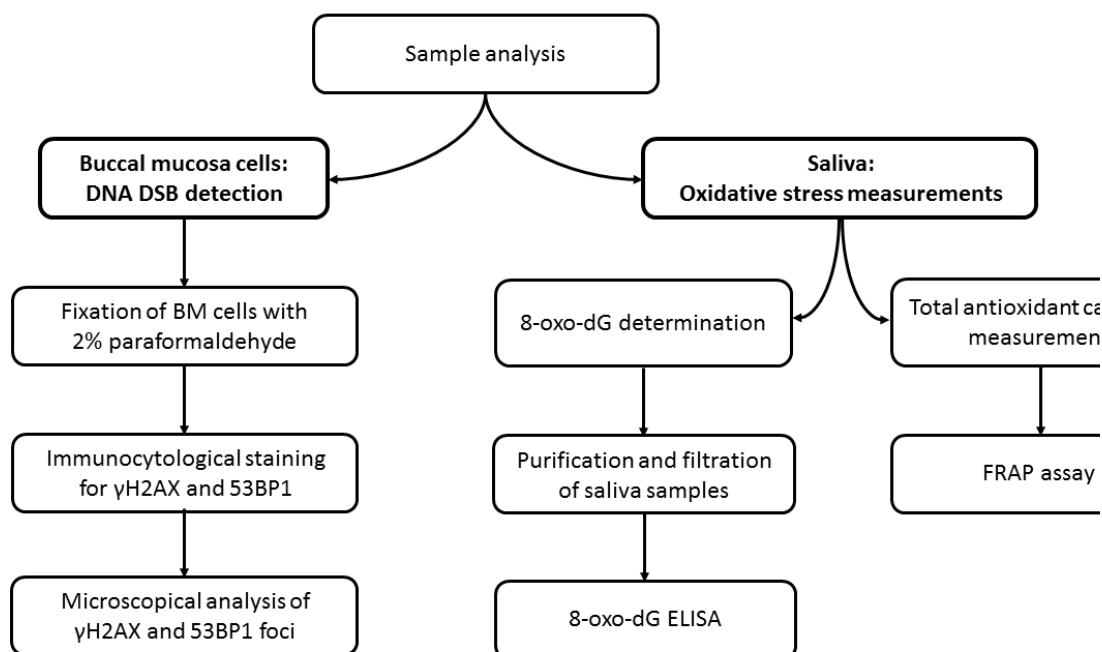
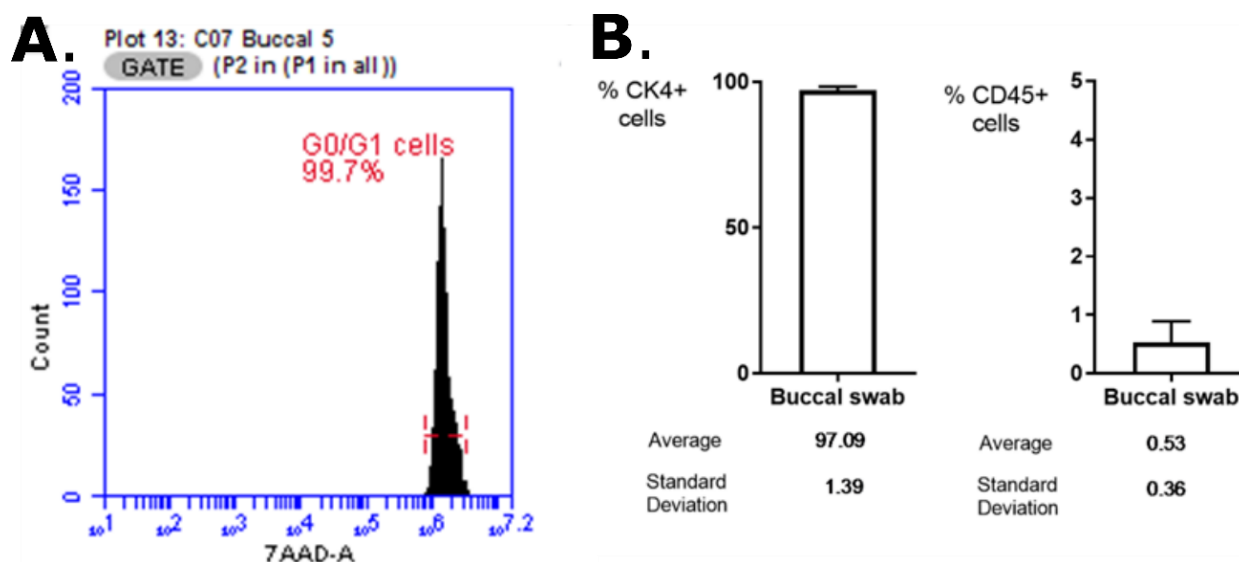


Figure 2. Flow chart for sample analysis. Schematic view of DNA double strand break detection in buccal mucosal cells and oxidative stress measurements in saliva samples. *DSB = Double-strand break; BM = Buccal mucosa; γH2AX = phosphorylated histone 2AX on Ser139; 53BP1 = p53-binding protein 1; 8-oxo-dG = 8-oxo-7,8-dihydro-2'-deoxyguanosine; FRAP = Ferric Reducing Antioxidant Power; ELISA = Enzyme-linked Immunosorbent assay*

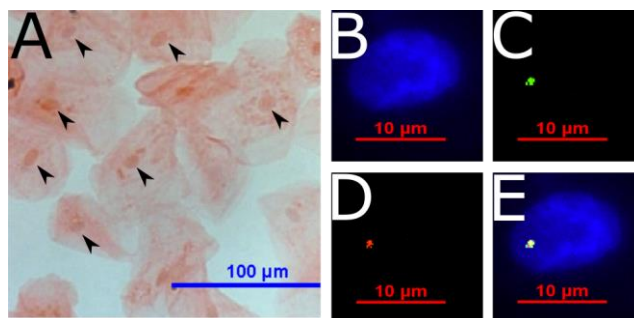
414



415

Figure 3. Flow cytometrical identification of cells collected by buccal swab. **A.** Overview of the cells that were in G_1/G_0 phase. Note that no S or G_2/M phase were observed, indicating that the cells are fully differentiated cells. **B.** Over 97% of the cells collected by buccal swab are CK4⁺ epithelial cells (= buccal cells), whereas less than 1% are CD45⁺, indicating that cells of hematological lineage are present (N = 6).

420



421

422 **Figure 4.** Microscopical identification of cells collected by buccal swab. **A.** Giemsa stain clearly shows nucleated
 423 epithelial cells (arrowheads), as well as unnucleated cells. This indicates that cells from all mucosal layers are
 424 collected. Enough nucleated cells are collected to perform immunocytochemistry. **B-E.** Buccal cells with DNA double
 425 strand break identified by colocalization of γ H2AX and 53BP1. **B.** Buccal cell nucleus, DAPI stain. **C.** γ H2AX-positive
 426 focus. **D.** 53BP1-positive focus. **E.** Merged image of B, D and E.

427

428 Tables

Table 1. Overview of scan parameters per patient included in this validation study.

Patient	Age	Sex	Device	Field of view	mAs	kV	Acquisition time (seconds)
1	57	Female	Newtom VGi evo	10x5	11	110	5
2	41	Female	Newtom VGi evo	10x5	6	110	5
3	30	Female	Newtom VGi evo	10x10	8	110	5
4	30	Male	Newtom VGi evo	10x10	10	110	5
5	71	Male	Newtom VGi evo	10x10	8	110	5
6	27	Female	Newtom VGi evo	10x10	8	110	5

mAs = milliamperage; kV = kilovoltage

429

430 Supplementary data

431 *Supplementary data 1*

432 Extension: PDF file.

433 Title: Patient questionnaire.

434 Description: Example of questionnaire that needs to be completed by the patient or the parents of the
435 patients upon entering the DIMITRA study. Data collected this way will be used to do analysis of age-,
436 gender-related effects.

437

438 *Supplementary data 2*

439 Extension: PDF file.

440 Title: Patient instructions

441 Description: Example of the instruction sheet handed to the patients during the informed consent
442 procedure.

443

444 **References**

- 445 1. Arai Y, Tammissalo E, Iwai K, Hashimoto K, Shinoda K. Development of a compact computed tomographic apparatus for
446 dental use. *Dentomaxillofac Radiol.* 1999;28(4):245-8.
- 447 2. Mozzo P, Procacci C, Tacconi A, Martini PT, Andreis IA. A new volumetric CT machine for dental imaging based on the
448 cone-beam technique: preliminary results. *European radiology.* 1998;8(9):1558-64.
- 449 3. Scarfe WC, Farman AG. What is cone-beam CT and how does it work? *Dent Clin North Am.* 2008;52(4):707-30, v.
- 450 4. Pauwels R. Cone beam CT for dental and maxillofacial imaging: dose matters. *Radiation protection dosimetry.*
451 2015;165(1-4):156-61.
- 452 5. Dawood A, Patel S, Brown J. Cone beam CT in dental practice. *British dental journal.* 2009;207(1):23-8.
- 453 6. Kapila SD, Nervina JM. CBCT in orthodontics: assessment of treatment outcomes and indications for its use.
454 *Dentomaxillofac Radiol.* 2015;44(1):20140282.
- 455 7. Scarfe WC, Farman AG, Levin MD, Gane D, Scarfe WC, Farman AG, et al. Essentials of maxillofacial cone beam computed
456 tomography - Clinical applications of cone-beam computed tomography in dental practice. *Alpha Omegan.* 2010;103(2):62-7.
- 457 8. De Vos W, Casselman J, Swennen GR. Cone-beam computerized tomography (CBCT) imaging of the oral and
458 maxillofacial region: a systematic review of the literature. *Int J Oral Maxillofac Surg.* 2009;38(6):609-25.
- 459 9. Feldkamp LA, Davis LC, Kress JW. Practical Cone-Beam Algorithm. *J Opt Soc Am A.* 1984;1(6):612-9.
- 460 10. Suomalainen A, Pakbaznejad Esmaeili E, Robinson S. Dentomaxillofacial imaging with panoramic views and cone beam
461 CT. *Insights Imaging.* 2015;6(1):1-16.
- 462 11. Shah N, Bansal N, Logani A. Recent advances in imaging technologies in dentistry. *World journal of radiology.*
463 2014;6(10):794-807.
- 464 12. Scarfe WC, Farman AG, Sukovic P. Clinical applications of cone-beam computed tomography in dental practice. *J Can*
465 *Dent Assoc.* 2006;72(1):75-80.
- 466 13. UNSCEAR. SOURCES AND EFFECTS OF IONIZING RADIATION. 2000;Volume II: Effects.
- 467 14. the UNSCo, Radiation EoA. UNSCEAR 2013 Report: Sources, effects and risks of ionizing radiation. 2013;II Annex B -
468 Effects of radiation exposure of children.
- 469 15. Ludlow JB, Davies-Ludlow LE, White SC. Patient risk related to common dental radiographic examinations: the impact of
470 2007 International Commission on Radiological Protection recommendations regarding dose calculation. *Journal of the*
471 *American Dental Association* (1939). 2008;139(9):1237-43.
- 472 16. Pauwels R, Beinsberger J, Collaert B, Theodorakou C, Rogers J, Walker A, et al. Effective dose range for dental cone beam
473 computed tomography scanners. *European journal of radiology.* 2012;81(2):267-71.
- 474 17. Oenning AC, Jacobs R, Pauwels R, Stratis A, Hedesiu M, Salmon B, et al. Cone-beam CT in paediatric dentistry: DIMITRA
475 project position statement. *Pediatr Radiol.* 2017.
- 476 18. Marcu M, Hedesiu M, Salmon B, Pauwels R, Stratis A, Oenning ACC, et al. Estimation of the radiation dose for pediatric
477 CBCT indications: a prospective study on ProMax3D. *Int J Paediatr Dent.* 2018.
- 478 19. Signorelli L, Patcas R, Peltomaki T, Schatzle M. Radiation dose of cone-beam computed tomography compared to
479 conventional radiographs in orthodontics. *Journal of orofacial orthopedics = Fortschritte der Kieferorthopadie : Organ/official*
480 *journal Deutsche Gesellschaft fur Kieferorthopadie.* 2016;77(1):9-15.
- 481 20. Li G. Patient radiation dose and protection from cone-beam computed tomography. *Imaging Sci Dent.* 2013;43(2):63-9.
- 482 21. Loubele M, Bogaerts R, Van Dijk E, Pauwels R, Vanheusden S, Suetens P, et al. Comparison between effective radiation
483 dose of CBCT and MSCT scanners for dentomaxillofacial applications. *European journal of radiology.* 2009;71(3):461-8.

- 484 22. Centre for Radiation CaEH. Guidance on the safe use of dental cone beam CT (computed tomography) equipment.
485 Oxfordshire: Health Protection Agency; 2010.
- 486 23. Theodorakou C, Walker A, Horner K, Pauwels R, Bogaerts R, Jacobs R. Estimation of paediatric organ and effective doses
487 from dental cone beam CT using anthropomorphic phantoms. *Br J Radiol.* 2012;85(1010):153-60.
- 488 24. Department of Public Health EaSDoHP-F, Women and Children's Health Cluster (FWC). Communicating radiation risks in
489 paediatric imaging - Information to support healthcare discussions about benefit and risk. Switzerland: World Health
490 Organization; 2016.
- 491 25. Brenner DJ, Hall EJ. Computed tomography--an increasing source of radiation exposure. *N Engl J Med.*
492 2007;357(22):2277-84.
- 493 26. RadiologyInfo.org. Radiation Dose in X-ray and CT exams. Accessed on 2018-12-06. Available from:
494 <https://www.radiologyinfo.org/en/pdf/safety-xray.pdf>.
- 495 27. Bogdanich W. CMJ. Radiation Worries for Children in Dentists' Chairs. *New York Times.* 2010.
- 496 28. Brenner DJ. Estimating cancer risks from pediatric CT: going from the qualitative to the quantitative. *Pediatr Radiol.*
497 2002;32(4):228-1; discussion 42-4.
- 498 29. Hall EJ. Lessons we have learned from our children: cancer risks from diagnostic radiology. *Pediatr Radiol.*
499 2002;32(10):700-6.
- 500 30. Berrington de Gonzalez A, Darby S. Risk of cancer from diagnostic X-rays: estimates for the UK and 14 other countries.
501 *Lancet.* 2004;363(9406):345-51.
- 502 31. UNSCEAR. SOURCES AND EFFECTS OF IONIZING RADIATION: UNSCEAR 2008 Report. New York: United Nations; 2010.
- 503 32. Holmberg O, Czarwinski R, Mettler F. The importance and unique aspects of radiation protection in medicine. *European*
504 *journal of radiology.* 2010;76(1):6-10.
- 505 33. D. K. Maurya TPAD. Role of Radioprotectors in the Inhibition of DNA Damage and Modulation of DNA Repair After
506 Exposure to Gamma-Radiation. In: Chen CC, editor. *Selected Topics in DNA Repair: InTech;* 2011.
- 507 34. Chapple IL, Matthews JB. The role of reactive oxygen and antioxidant species in periodontal tissue destruction.
508 *Periodontol 2000.* 2007;43:160-232.
- 509 35. Tothova L, Kamodyova N, Cervenka T, Celec P. Salivary markers of oxidative stress in oral diseases. *Front Cell Infect*
510 *Microbiol.* 2015;5:73.
- 511 36. Cooke MS, Evans MD, Dizdaroglu M, Lunec J. Oxidative DNA damage: mechanisms, mutation, and disease. *FASEB J.*
512 2003;17(10):1195-214.
- 513 37. Kasai H, Nishimura S. Hydroxylation of deoxy guanosine at the C-8 position by polyphenols and aminophenols in the
514 presence of hydrogen peroxide and ferric ion. *Gan.* 1984;75(7):565-6.
- 515 38. Lobrich M, Shibata A, Beucher A, Fisher A, Ensminger M, Goodarzi AA, et al. gammaH2AX foci analysis for monitoring
516 DNA double-strand break repair: strengths, limitations and optimization. *Cell cycle (Georgetown, Tex).* 2010;9(4):662-9.
- 517 39. Dugle DL, Gillespie CJ, Chapman JD. DNA strand breaks, repair, and survival in x-irradiated mammalian cells. *Proc Natl*
518 *Acad Sci U S A.* 1976;73(3):809-12.
- 519 40. Olive PL. The role of DNA single- and double-strand breaks in cell killing by ionizing radiation. *Radiat Res.* 1998;150(5
520 Suppl):S42-51.
- 521 41. Jackson SP. Sensing and repairing DNA double-strand breaks. *Carcinogenesis.* 2002;23(5):687-96.
- 522 42. Richardson C, Jasin M. Frequent chromosomal translocations induced by DNA double-strand breaks. *Nature.*
523 2000;405(6787):697-700.
- 524 43. Vamvakas S, Vock EH, Lutz WK. On the role of DNA double-strand breaks in toxicity and carcinogenesis. *Crit Rev Toxicol.*
525 1997;27(2):155-74.
- 526 44. Khanna KK, Jackson SP. DNA double-strand breaks: signaling, repair and the cancer connection. *Nat Genet.*
527 2001;27(3):247-54.
- 528 45. Kinner A, Wu W, Staudt C, Iliakis G. Gamma-H2AX in recognition and signaling of DNA double-strand breaks in the
529 context of chromatin. *Nucleic Acids Res.* 2008;36(17):5678-94.
- 530 46. Riches LC, Lynch AM, Gooderham NJ. Early events in the mammalian response to DNA double-strand breaks.
531 *Mutagenesis.* 2008;23(5):331-9.
- 532 47. Ciccio A, Elledge SJ. The DNA damage response: making it safe to play with knives. *Mol Cell.* 2010;40(2):179-204.
- 533 48. Torres-Bugarin O, Zavala-Cerna MG, Nava A, Flores-Garcia A, Ramos-Ibarra ML. Potential uses, limitations, and basic
534 procedures of micronuclei and nuclear abnormalities in buccal cells. *Dis Markers.* 2014;2014:956835.
- 535 49. Spivack SD, Hurteau GJ, Jain R, Kumar SV, Aldous KM, Gierthy JF, et al. Gene-environment interaction signatures by
536 quantitative mRNA profiling in exfoliated buccal mucosal cells. *Cancer Res.* 2004;64(18):6805-13.
- 537 50. Thomas P, Holland N, Bolognesi C, Kirsch-Volders M, Bonassi S, Zeiger E, et al. Buccal micronucleus cytome assay. *Nat*
538 *Protoc.* 2009;4(6):825-37.
- 539 51. Siddiqui MS, Francois M, Fenech MF, Leifert WR. gammaH2AX responses in human buccal cells exposed to ionizing
540 radiation. *Cytometry A.* 2015;87(4):296-308.
- 541 52. Sarto F, Tomanin R, Giacomelli L, Iannini G, Cupiraggi AR. The micronucleus assay in human exfoliated cells of the nose
542 and mouth: application to occupational exposures to chromic acid and ethylene oxide. *Mutat Res.* 1990;244(4):345-51.
- 543 53. Lee JM, Garon E, Wong DT. Salivary diagnostics. *Orthod Craniofac Res.* 2009;12(3):206-11.
- 544 54. Mandel ID. Salivary diagnosis: more than a lick and a promise. *Journal of the American Dental Association (1939).*
545 1993;124(1):85-7.
- 546 55. Miller SM. Saliva testing--a nontraditional diagnostic tool. *Clin Lab Sci.* 1994;7(1):39-44.
- 547 56. Dame ZT, Aziat F, Mandal R, Krishnamurthy R, Bouatra S, Borzouie S, et al. The human saliva metabolome. *Metabolomics.*
548 2015;11(6):1864-83.
- 549 57. ICRP. Recommendations of the ICRP. ICRP Publication 26. 1977(Ann. ICRP 1 (3)).

- 550 58. ICRP. 1990 Recommendations of the International Commission on Radiological Protection. ICRP Publication 60.
551 1991(Ann. ICRP 21 (1-3)).
- 552 59. ICRP. The 2007 Recommendations of the International Commission on Radiological Protection. ICRP Publication 103.
553 2007(Ann. ICRP 37 (2-4)).
- 554 60. Stratis A. Customized Monte Carlo Modelling for Paediatric Patient Dosimetry in Dental and Maxillofacial Cone Beam
555 Computed Tomography Imaging [Doctoral Thesis]. Leuven University Press: KU Leuven; 2018.
- 556 61. Virag P, Hedesiu M, Soritau O, Perde-Schrepler M, Brie I, Pall E, et al. Low-dose radiations derived from cone-beam CT
557 induce transient DNA damage and persistent inflammatory reactions in stem cells from deciduous teeth. *Dentomaxillofac Radiol.*
558 2018;20170462.
- 559 62. Suetens A, Konings K, Moreels M, Quintens R, Verslegers M, Soors E, et al. Higher Initial DNA Damage and Persistent Cell
560 Cycle Arrest after Carbon Ion Irradiation Compared to X-irradiation in Prostate and Colon Cancer Cells. *Front Oncol.* 2016;6:87.
- 561 63. Ghardi M, Moreels M, Chatelain B, Chatelain C, Baatout S. Radiation-induced double strand breaks and subsequent
562 apoptotic DNA fragmentation in human peripheral blood mononuclear cells. *Int J Mol Med.* 2012;29(5):769-80.
- 563 64. Baselet B, Belmans N, Coninx E, Lowe D, Janssen A, Michaux A, et al. Functional Gene Analysis Reveals Cell Cycle Changes
564 and Inflammation in Endothelial Cells Irradiated with a Single X-ray Dose. *Front Pharmacol.* 2017;8:213.
- 565 65. Schindelin J, Arganda-Carreras I, Frise E, Kaynig V, Longair M, Pietzsch T, et al. Fiji: an open-source platform for
566 biological-image analysis. *Nat Methods.* 2012;9(7):676-82.
- 567 66. De Vos WH, Van Neste L, Dieriks B, Joss GH, Van Oostveldt P. High content image cytometry in the context of
568 subnuclear organization. *Cytometry A.* 2010;77(1):64-75.
- 569 67. Munro CL, Grap MJ, Jablonski R, Boyle A. Oral health measurement in nursing research: state of the science. *Biol Res*
570 *Nurs.* 2006;8(1):35-42.
- 571 68. Shakeri Manesh S, Sangsuwan T, Pour Khavari A, Fotouhi A, Emami SN, Haghdoost S. MTH1, an 8-oxo-2'-
572 deoxyguanosine triphosphatase, and MYH, a DNA glycosylase, cooperate to inhibit mutations induced by chronic exposure to
573 oxidative stress of ionising radiation. *Mutagenesis.* 2017;32(3):389-96.
- 574 69. Haghdoost S, Czene S, Naslund I, Skog S, Harms-Ringdahl M. Extracellular 8-oxo-dG as a sensitive parameter for
575 oxidative stress in vivo and in vitro. *Free Radic Res.* 2005;39(2):153-62.
- 576 70. Vandevoorde C, Gomolka M, Roessler U, Samaga D, Lindholm C, Fernet M, et al. EPI-CT: in vitro assessment of the
577 applicability of the gamma-H2AX-foci assay as cellular biomarker for exposure in a multicentre study of children in diagnostic
578 radiology. *Int J Radiat Biol.* 2015;91(8):653-63.
- 579 71. El-Saghire H, Thierens H, Monsieurs P, Michaux A, Vandevoorde C, Baatout S. Gene set enrichment analysis highlights
580 different gene expression profiles in whole blood samples X-irradiated with low and high doses. *Int J Radiat Biol.* 2013;89(8):628-
581 38.
- 582 72. Sudprasert W, Navasumrit P, Ruchirawat M. Effects of low-dose gamma radiation on DNA damage, chromosomal
583 aberration and expression of repair genes in human blood cells. *Int J Hyg Environ Health.* 2006;209(6):503-11.
- 584 73. Ponzinibbio MV, Crudeli C, Peral-Garcia P, Seoane A. Low-dose radiation employed in diagnostic imaging causes genetic
585 effects in cultured cells. *Acta Radiol.* 2010;51(9):1028-33.
- 586 74. Das Roy L, Giri S, Singh S, Giri A. Effects of radiation and vitamin C treatment on metronidazole genotoxicity in mice.
587 *Mutat Res.* 2013;753(2):65-71.
- 588 75. Ainsbury EA, Al-Hafidh J, Bajinskis A, Barnard S, Barquinero JF, Beinke C, et al. Inter- and intra-laboratory comparison of a
589 multibiodosimetric approach to triage in a simulated, large scale radiation emergency. *Int J Radiat Biol.* 2014;90(2):193-202.
- 590 76. Sangsuwan T, Haghdoost S. The nucleotide pool, a target for low-dose gamma-ray-induced oxidative stress. *Radiat Res.*
591 2008;170(6):776-83.
- 592 77. Tsuzuki T, Nakatsu Y, Nakabeppu Y. Significance of error-avoiding mechanisms for oxidative DNA damage in
593 carcinogenesis. *Cancer Sci.* 2007;98(4):465-70.
- 594 78. Magnander K, Elmroth K. Biological consequences of formation and repair of complex DNA damage. *Cancer letters.*
595 2012;327(1-2):90-6.
- 596 79. Kryston TB, Georgiev AB, Pissis P, Georgakilas AG. Role of oxidative stress and DNA damage in human carcinogenesis.
597 *Mutat Res.* 2011;711(1-2):193-201.
- 598 80. Gonzalez JE, Roch-Lefevre SH, Mandina T, Garcia O, Roy L. Induction of gamma-H2AX foci in human exfoliated buccal
599 cells after in vitro exposure to ionising radiation. *Int J Radiat Biol.* 2010;86(9):752-9.
- 600 81. Vandevoorde C, Vral A, Vandekerckhove B, Philippe J, Thierens H. Radiation Sensitivity of Human CD34(+) Cells Versus
601 Peripheral Blood T Lymphocytes of Newborns and Adults: DNA Repair and Mutagenic Effects. *Radiat Res.* 2016;185(6):580-90.
- 602 82. Deminice R, Sicchieri T, Payao PO, Jordao AA. Blood and salivary oxidative stress biomarkers following an acute session
603 of resistance exercise in humans. *Int J Sports Med.* 2010;31(9):599-603.
- 604 83. da Fonte JBM, de Andrade TM, Albuquerque RLC, de Melo MDB, Takeshita WM. Evidence of genotoxicity and
605 cytotoxicity of X-rays in the oral mucosa epithelium of adults subjected to cone beam CT. *Dentomaxillofac Rad.* 2018;47(2).
- 606 84. de Geus JL, Wambier LM, Bortoluzzi MC, Loguercio AD, Kossatz S, Reis A. Does smoking habit increase the micronuclei
607 frequency in the oral mucosa of adults compared to non-smokers? A systematic review and meta-analysis. *Clin Oral Investig.*
608 2018;22(1):81-91.